Acta Cryst. (1986). B42, 78-84

Structures of Ethane, Hexamethylethane* and Hexamethyldisilane in their Plastic Phases

BY J. P. AMOUREUX, M. FOULON, M. MULLER AND M. BEE

Laboratoire de Dynamique des Cristaux Moléculaires (UA 801 CNRS), Université des Sciences et Techniques de Lille, 59655 Villeneuve d'Ascq CEDEX, France

(*Received* 12 *September* 1984; *accepted* 2 *July* 1985)

Abstract

The plastic structures of three similar compounds: ethane, hexamethylethane (HME) and hexamethyldisilane (HMDS) are analysed. The unit cells are body-centred cubic, space group $Im3m$, $Z=2$. Two different methods are employed: a Frenkel model and a decomposition of the molecular orientational probability on symmetry-adapted functions. The molecules can occupy four different equilibrium positions in which the molecular and lattice threefold axes are aligned. Around these $\langle 111\rangle$ axes there exists only one equilibrium position, the six lateral C atoms (or H atoms for ethane) being in the $(1\bar{1}0)$ planes, close to the $\langle 001\rangle$ axes. In the case of HME, the refinements are always slightly better for the CALDER conformation than for the LEM one.

I. Introduction

Because of their softness, sublimability, or low melting point, some compounds have to be grown directly on the automatic X-ray diffractometer. This '*in situ*' crystallization technique has been developed in our laboratory and employed for three similar molecular crystals: ethane (C_2H_6), hexamethylethane [$C_2(CH_3)_6$: HME], and hexamethyldisilane [$Si_2(CH_3)_6$: HMDS].

A structural analysis of the two solid phases of ethane has already been published (Van Nes & Vos, 1978). The low-temperature phase crystallizes in the monoclinic space group $P2_1/n$. However, the analysis of the plastic phase does not seem conclusive: the two different models are refined with six parameters for only twelve independent Bragg peaks and give a C—C bond of 1·41 Å.

Unlike ethane, the plastic phase of HME extends over a very wide temperature range (Table 1). When the temperature increases, the molecular orientational probability of this compound changes continuously from very localized at the transition to quasi-isotropic at the melting point. The study of HMDS has been carried out in a parallel way to that of HME; we expect to characterize the relations of the inertial molecular tensor anisotropy with their dynamical properties.

* IUPAC name: 2,2,3,3-tetramethylbutane.

Table 1. *Temperatures and enthalpies for the solid–solid transitions (T_t) and the melting points (T_m)*

	T_t(K)	H_t(kJ mol^{-1})	T_m(K)	H_m(kJ mol^{-1})
Ethane (*a*)	89·82 (2)	2·14	90·27 (2)	0·58
HME (*b*)	152·5	1·56	373·8	2·42
HMDS (*c*)	221·7	5·25	287·7	1·25

(*a*) Eggers (1975). (*b*) Scott, Douslin, Gross, Oliver & Huffman (1952). (*c*) Suga & Seki (1959).

II. Experimental conditions

(1) *Crystallization and thermal treatment*

Non-porous quartz capillaries 0·3 mm in diameter were filled with these compounds and vacuum sealed. All the thermal treatments during crystallization were performed directly on the X-ray diffractometer using a nitrogen gas flow (Leybold apparatus).

(*a*) *Ethane.* It should be pointed out that the monoclinic cell has two parameters nearly equal to the cubic one; therefore, the (011) monoclinic and cubic Bragg reflections will have nearly the same θ diffraction angle. This peak observed during the thermal treatment will give information on the quality of the sample in each phase.

A cubic single crystal was grown from a small plastic germ obtained through the following procedure (Muller, 1981):

(i) Starting with a polycrystalline monoclinic sample obtained by cooling to 85 K, we first increased the temperature very slowly to as near the melting point as possible. In the plastic phase, the (011) Bragg peak was alone but very wide.

(ii) When this peak almost completely disappeared, the small intensity still observed was assumed to correspond to a monocrystalline plastic germ.

(iii) The temperature was then lowered to 90·05 (10) K in 0·05 K steps, an accuracy required by the small temperature range of the plastic phase (0·45 K).

Recorded Bragg peaks were all unique and of width 0·15° (FWHM), showing the good quality of the single crystal. The cubic lattice parameter is $a=5{\cdot}307$ (3) Å.

(*b*) *HME.* Single crystals of HME were obtained '*in situ*' by slow sublimation at a cold point created with a temperature gradient along the capillary between 282 and about 290 K.

0108-7681/86/010078-07$01.50

The structure of HME was recorded at four temperatures: 282, 242, 201 and 172 K. An accurate measure of the lattice parameter from 155 K to 293 K fits in well with that deduced previously above room temperature (Seyer, Bennet & Williams, 1949) (Fig. 1). When cooling from the plastic phase, the transition to the ordered phase appeared at $153 \pm 1{\cdot}5$ K. The crystal did not shatter but was composed of domains. On reheating, the Bragg peaks of the cubic phase had a width of 0·5° (FWHM), to be compared to the 0·15° observed before this thermal treatment.

(*c*) *HMDS.* Single crystals of HMDS were grown directly '*in situ*' on the diffractometer in a similar way to ethane, using the Bridgman method. The cubic structure [$a = 8{\cdot}426$ (5) Å] was only recorded at 225 K because of the softness of this compound at higher temperature. Bragg reflections were composed of a unique peak of width 0·30° (FWHM). A very important delay to the transition may exist when the temperature is decreased: the crystal only shattered at 200 K.

For these last two compounds, we noticed that the mosaicity of the single crystals decreased slowly after they had been grown, certainly owing to the molecular self-diffusion in the lattice, as pointed out by NMR experiments (Albert, Gutowsky & Ripmeester, 1972; Chadwick, Chezeau, Folland, Forrest & Strange, 1975).

(2) *Data collection and weighting scheme*

We used an automatic X-ray diffractometer (Philips PW 1100) with Mo $K\bar{\alpha}$ radiation ($\lambda = 0{\cdot}7107$ Å) and a 0·8 mm ∅ collimator. θ–2θ scans were used with speeds of 0·009° min^{-1} and fixed scan widths of 1·30°.

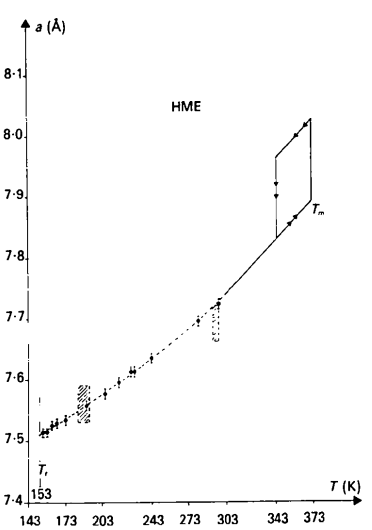

Fig. 1. Lattice parameter *a versus* temperature. The continuous line (above 300 K) has been measured by dilatometry (Seyer *et al.*, 1949). The upper line between 347 K and T_m is only observed when the temperature is decreased from the liquid phase. The two large error rectangles at 295 and 188 K represent the values measured by Reynolds (1979) on Weissenberg photographs.

For the three molecular crystals the system is body-centred cubic with $Z = 2$. The condition $F_o(h, k, l) = F_o(\bar{k}, h, l)$ was always verified and allowed us to reject the space groups $Im3$ and $I23$. Therefore, if we take into account the D_{3h} molecular symmetry, only one space group is possible: $Im3m$.

For the three compounds several hundreds of diffraction peaks were measured of which only 9 independent reflections were retained ($F_o/\sigma \geq 3$) for ethane, 17 for HMDS, and 30-34-40-52 for HME (respectively at 282-242-201-172 K).

In order to be sure that secondary extinction did not occur, comparisons of strong reflections for two different crystals were performed for HME and HMDS. Within 5%, the experimental intensities were always in the same ratio for the two crystals of each compound, and hence no extinction corrections were applied. The low absorption coefficients rule out corrections.

In plastic crystals, there are always some Bragg reflections whose intensities are very strong compared to the others. Therefore a weighting scheme is needed to use all the experimental data. We have tried to minimize the weighted R factor:

$$wR^2 = \sum |F_o - |F_c||^2 \sigma^{-2} / \sum F_o^2 \sigma^{-2}$$
$$R = \sum |F_o - |F_c|| / \sum F_o, \quad (1)$$

with $\sigma^2 = \sigma_c^2 + E^2 F_o^2$. σ_c is the standard deviation from counting. E is a constant value chosen so that wR and the classical R factor are nearly equal. According to this condition the best E values were 0·02 for ethane and HME and 0·005 for HMDS.*

III. Structural modes

Structural analysis of plastic crystals can be carried out either with a Frenkel model, or with the decomposition of the atomic orientational average density on symmetry-adapted functions.

(1) *Molecular description*

In the following, we shall consider the molecules as rigid, as verified for HME by Raman diffusion (Gharby, Sauvajol, Fontaine & More, 1985). Whatever the method used, the atoms are first defined with respect to a molecular referential whose Oz axis is the molecular threefold axis (called the Δ axis) (Fig. 2). One can describe the molecules of HME and HMDS with only five parameters ($d, d', \alpha', d'', \alpha''$) and that of ethane with three parameters (d, d', α'); these were fixed at the usual values (within 1%). The D_{3h} symmetry of the HME and HMDS molecules

* Lists of structure factors and anisotropic thermal parameters have been deposited with the British Library Lending Division as Supplementary Publication No. SUP 42323 (4 pp.). Copies may be obtained through The Executive Secretary, International Union of Crystallography, 5 Abbey Square, Chester CH1 2HU, England.

allows two different conformations known as LEM and CALDER. They correspond to each other by a 60° rotation of the methyl groups around the C–C or Si–C axes. In the case of HME, we shall call the central C atoms those placed on Δ, and the six other C atoms lateral. As explained below, the structural refinements showed that the Δ axis always coincides with the ⟨111⟩ axes (four equilibrium positions).

In this case, when H atoms of ethane (or lateral C atoms of HME and HMDS) lie in the $(1\bar{1}0)$ planes, the molecule can occupy two positions called *A* and *B* in the following, corresponding to H atoms (or lateral C atoms) close to the ⟨001⟩ or ⟨110⟩ axes, respectively.

(2) *Frenkel model*

In this model, atoms are fixed at well defined equilibrium positions: their orientational probabilities are Dirac δ functions. The effect of thermal motions on the structure factors is taken into account with a Debye–Waller temperature factor, $\exp(-W)$. This description assumes the harmonicity of the thermal motions and is therefore only suitable when they are of small amplitude.

For each equilibrium position, the temperature factor $\exp(-W)$ is calculated with two symmetrical tensors: **T** (translations) and **L** (librations). These two tensors **T** and **L** must take into account the molecular symmetry and the local order produced by the neighbouring molecules.

Therefore, assuming that the time-averaged local order has C_3 uniaxial symmetry around the Δ threefold molecular axis, we have to apply D_{3h} symmetry to the **T** and **L** tensors, which are reduced to four mean-square amplitudes:

$L_\parallel$ for librations of the molecule around the Δ axis;
$L_\perp$ for librations perpendicular to the Δ axis;
$T_\parallel$ for translations along the Δ axis;

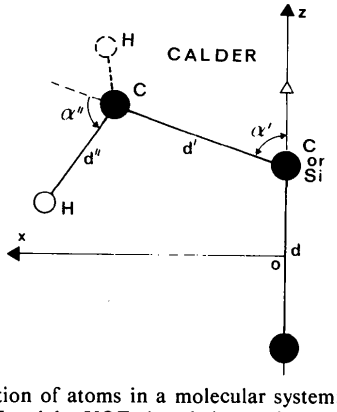

Fig. 2. Description of atoms in a molecular system: Δ threefold axis along *OZ* and the *XOZ* plane being a mirror. The molecular system used with the symmetry-adapted functions is obtained from this figure, by a 30° rotation around *OZ*. C or Si atoms are in black and H atoms in white. The LEM conformation corresponds to $\alpha'' = -70{\cdot}5°$.

$T_\perp$ for translations along any axis perpendicular to the former.

The *W* factor is then expressed as follows:

$$W/2\pi^2 = X_\parallel^2 T_\parallel + X_\perp^2 T_\perp + (\mathbf{X}\wedge\mathbf{M})_\parallel^2 L_\parallel + (\mathbf{X}\wedge\mathbf{M})_\perp^2 L_\perp, \quad (2)$$

where **M** is the vector joining each atom to the origin of the crystal lattice; **X** is the scattering vector; $X_\parallel$, $(\mathbf{X}\wedge\mathbf{M})_\parallel$, $X_\perp$ and $(\mathbf{X}\wedge\mathbf{M})_\perp$ are the components of **X** and $\mathbf{X}\wedge\mathbf{M}$ respectively along and perpendicular to the molecular threefold axis (Δ).

When thermal motions are isotropic, there exist only two different isotropic mean-square amplitudes. We shall write them T_i and L_i:

$$T_i = T_\perp = T_\parallel, \qquad L_i = L_\perp = L_\parallel. \quad (3)$$

We have taken into account the shortening effect arising from the librations. The relative shortening $\Delta M/M$ of the interatomic distances is equal to $L_i(\text{rad}^2)$ when thermal motions can be considered as isotropic.

(3) *Symmetry-adapted function analysis*

In this method (Amoureux, Sauvajol & Bee, 1981), the averaged probability that a molecule will be in a particular orientation with respect to the crystal axes is expanded on rotator functions. The $A^l_{mm'}$ coefficients of this expansion are introduced as parameters in the refinements. If we take into account the molecular (D_{3h}) and lattice (cubic) symmetries, the non-zero $A^l_{mm'}$ terms up to order 10 correspond to $l = 4, 6, 8, 10$ and $m = 1$.

These coefficients can be separated into two groups:

(i) the A^l_{11} which fix the orientation of the molecular Δ axis;

(ii) the other $A^l_{1m'}$ terms ($m' \neq 1$) which determine the molecular orientation around the Δ axis. These terms are all equal to zero for a cylindrical probability around this Δ axis.

The free isotropic rotation corresponds to the zeroth order only ($A^0_{11} = 1$). For each *l* order, the number of determinable $A^l_{mm'}$ terms is always lower than, or equal to, the number of 'independent' atomic shells describing the molecule (Prandl, 1981). Two different shells are 'independent' if the atoms of these two shells do not correspond to the same polar angles in the molecular system. The total number of different shells is two in ethane and four in HME and HMDS. However, in these last two compounds, averaged H atoms, the C atoms to which they are bound and the origin of the molecular system are nearly aligned. This approximation is all the more exact as the H scattering factor is small in X-ray experiments. One can then only expect two or three $A^l_{mm'}$ parameters to be refined for each order *l*. In a first approximation, we neglected the translation–rotation coupling and we used an isotropic translational amplitude T_i.

Table 2. *Translational and librational thermal parameters refined with a Frenkel model*

Compound	Conformation	Position	wR(%)	R(%)	T_i(Å^2)	$T_\parallel$(Å^2)	$T_\perp$(Å^2)	$\sqrt{L_i}$(°)
Ethane (90·05 K)		*B*	12·1	11·8	0·19 (4)			23 (5)
		A	7·3	9·2	0·18 (2)			22 (3)
HMDS (225 K)		*B*	29	34	0·25 (8)			10 (5)
		A	5·1	5·1	0·28 (2)			13 (2)
		A	4·4	5·1		0·32 (3)	0·26 (3)	14 (2)
HME (172 K)	CALDER	*B*	42					
		A+*B*	23					
	LEM		7·9	5·1	0·060 (2)			8·0 (3)
	LEM+CALDER		5·5	4·9	0·061 (1)			7·5 (3)
	CALDER		4·3	4·1	0·061 (1)			7·5 (2)
			3·5	3·3		0·052 (3)	0·066 (3)	
HME (201 K)	CALDER	*A*	4·7	4·4	0·073 (2)			8·8 (2)
			4·3	3·6		0·064 (5)	0·077 (5)	
HME (242 K)	CALDER		5·8	5·3	0·095 (3)			10·2 (2)
HME (282 K)	CALDER		6·9	6·2	0·117 (6)			11·0 (3)

Table 3. *$A^l_{1m'}$ and T_i parameters, refined with symmetry-adapted functions and the CALDER conformation for HME and HMDS*

The theoretical values corresponding to the molecule fixed without librations at its *A* equilibrium positions are indicated on the first line ($A^8_{11}=0{\cdot}21$, $A^{10}_{11}=-0{\cdot}65$).

Compound	wR(%)	R(%)	T_i(Å^2)	$-A^4_{11}$	A^6_{11}	A^4_{12}	A^6_{12}	$-A^6_{13}$	$-A^8_{13}$	$-A^{10}_{13}$
Molecule fixed in position *A* without librations				0·51	0·63	0·86	0·54	0·56	0·75	0·45
Ethane	5·3	8·7	0·19 (1)							
(90·05 K)	2·4	4·1	0·197 (8)	0·50 (6)						
	2·0	3·9	0·201 (6)	0·59 (5)	0·44 (8)					
HMDS	13·5	14·2	0·33 (6)							
(225 K)	6·9	8·1	0·35 (4)	0·70 (30)						
	5·8	7·1	0·32 (4)	0·65 (15)	0·50 (20)					
HME	17	13	0·14	0·62	0·93					
(172 K)	5·3	3·4	0·062 (2)	0·361 (17)	0·40 (9)	0·817 (27)	0·371 (20)	0·54 (10)	0·73 (3)	0·162 (14)
HME (201 K)	4·1	2·6	0·071 (3)	0·350 (18)	0·35 (10)	0·756 (27)	0·331 (21)	0·48 (10)	0·66 (3)	0·132 (14)
HME (242 K)	2·4	1·8	0·095 (2)	0·330 (13)	0·30 (10)	0·651 (26)	0·274 (18)	0·43 (5)	0·52 (3)	0·100 (11)
HME (282 K)	1·9	1·6	0·112 (2)	0·291 (15)	0·24 (10)	0·601 (23)	0·206 (25)	0·38 (5)	0·44 (2)	0·50 (12)

IV. Structures of ethane and HMDS

(1) *Frenkel model* (*Table* 2)

In these two compounds, the molecules are localized in the *A* positions. In ethane the relatively small difference in wR (4·8%) between the two positions *A* and *B* arises from the fact that they differ only in the positions of the H atoms. The use of an anisotropic Debye–Waller factor does not bring a significant reduction of wR.

In HMDS, the very important translational amplitude (63 K below the melting point) corresponds to the very important molecular self-diffusion observed in NMR (Albert *et al.*, 1972), certainly increased by about 2% of impurities (probably hexamethyldisiloxane). The use of an anisotropic Debye–Waller factor shows a small anisotropy in the translational term. The small number (17) of observed independent Bragg peaks does not allow LEM or CALDER conformations to be distinguished.

(2) *Symmetry-adapted functions* (*Table* 3)

The relatively small wR value (particularly for ethane) refined with a free isotropic rotational model ($A^l_{mm'}=\delta_{l,0}$) is a confirmation of the large librational amplitude. With both compounds a good description is obtained with a constant cylindrical charge density (only $A^l_{11}\neq 0$) up to order 6. The small number of measured independent reflections limits the number of parameters.

The $C(\Delta)$ orientational probabilities of the molecular Δ axes [Amoureux *et al.*, 1981; equation (22)] are very similar for the two compounds and they show (Fig. 3) that the equilibrium positions are well aligned along the ⟨111⟩ axes.

V. Structure of HME

(1) *Frenkel model* (*Table* 2)

(a) Equilibrium positions and molecular conformation. In order to define precisely the equilibrium posi-

tions and the conformation in the plastic phase of HME, we first analysed the experimental data recorded at 172 K (maximum number of observed Bragg peaks: 52).

The refinements clearly show that there exists only one equilibrium position (A) around the molecular Δ axis. In the following, with the Frenkel model, we always used this A position in the refinements. We then tried to determine the H positions by introducing either 6 equilibrium positions around the C–C bond (conformation LEM + CALDER) or only 3 (LEM or CALDER). According to the best refinements it seems that the CALDER conformation is the most probable. Consequently, in the solid phase of this compound the rotations of methyl and *tert*-butyl groups would both be of order 3. Whatever the model used, whether Frenkel or with symmetry-adapted functions, the best refinements have always been obtained for the CALDER conformation. However, the wR value with the LEM conformation draws nearer the CALDER one as the temperature increases, and they are nearly equal at 282 K. In the following, we shall only give the results concerning the CALDER conformation.

(*b*) *Variations of the thermal parameters with temperature.* We then carried out the refinements corresponding to the four experimental temperatures with an isotropic Debye–Waller factor. Table 2 reporting the different results shows that the lower the temperature, the more suitable the Frenkel model. Indeed, the wR factor decreases with temperature in spite of the increasing number of independent measured Bragg peaks. The variation of T_i is almost proportional to the temperature, but that of L_i is not (Fig. 4). This effect is certainly correlated to the fact that the isotropic molecular tumbling between the ⟨111⟩ axes is very slow at 172 K and becomes very fast for a small increase of temperature (Bee, 1985). This L_i term would then partially reflect the release of this isotropic reorientation. The use of an anisotropic Debye–Waller factor only sensibly improves the refinements at 172 and 201 K. The amplitude of the translational thermal motions is a little smaller along the molecular Δ axis than it is perpendicular to it. However, even for these low temperatures, the two $L_\parallel$ and $L_\perp$ values stay equal to the previous L_i value.

(2) *Symmetry-adapted functions* (*Table* 3)

(*a*) $A^l_{mm'}$ *parameters introduced in the refinements.* As for the Frenkel model, we first analysed the experimental data recorded at 172 K introducing the CALDER conformation. Initially, we used a constant spherical charge density, but the agreement was very poor: $wR = 64\%$. A refinement with a free cylindrical density leads to A^l_{11} values (Table 3) fitting in well with aligned molecular Δ and lattice ⟨111⟩ threefold axes. However, the high final wR value (17%) indicates that the molecular uniaxial rotation is not free but strongly hindered. We had then to modulate the molecular orientational probability around the Δ axis and then to refine the other $A^l_{1m'}$ ($m' \neq 1$) parameters. There exist '*a priori*' too many parameters (12 up to order 10) and we know that only two or three of them can be deduced at each l level from the refinements.

We then had to set aside the $A^l_{1m'}$ parameters which have negligible influence on the refinements. All these trials were processed using as initial $A^l_{1m'}$ values in the refinements those deduced from the equilibrium positions with the Frenkel model. The functions adapted to D_{3h} symmetry may have small values for some atoms of this particular molecule. This would then correspond to unrefinable $A^l_{1m'}$ terms. This is the case at orders 8 and 10 for the lateral C atoms and, therefore, only the two central ones fix the A^8_{11} and A^{10}_{11} parameters which were then eliminated, their determination needing Bragg peaks with $h^2+k^2+l^2 \geq 300$ (Amoureux *et al.*, 1981).

For similar reasons one can see in Table 3 that A^6_{11} and A^6_{13} are not accurately defined. When a LEM conformation is used with the same $A^l_{1m'}$ parameters, the results are very similar, but $wR = 6{\cdot}1\%$ and $R = 4{\cdot}1\%$.

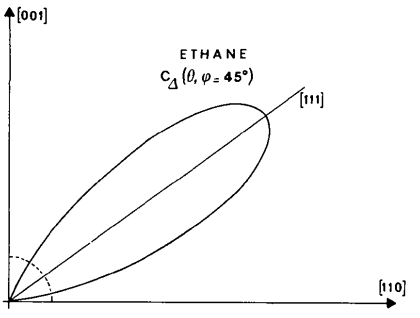

Fig. 3. Orientational probability in a $(1\bar{1}0)$ plane for the Δ molecular threefold axis of ethane. The circle corresponds to the value $\frac{1}{4}\pi$ for a completely random distribution of orientations.

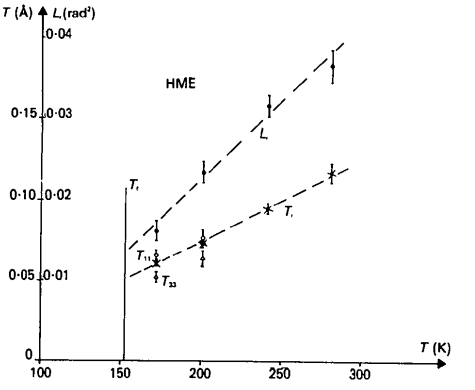

Fig. 4. Isotropic thermal parameters deduced from the Frenkel model: L_i(●) and T_i(×). The anisotropic translational parameters are only represented at 172 and 201 K when they differ from T_i: $T_\perp$(○) and $T_\parallel$(△).

(*b*) *Variations with temperature of the* $A^l_{1m'}$ *parameters.* In a second stage, we carried out the refinements corresponding to the other three experimental temperatures, with the same eight parameters. As it was foreseeable, contrary to the Frenkel model, this method is more and more suitable as the temperature increases and the molecular orientational probability is less localized. When the temperature decreases, the $|A^l_{mm'}|$ terms increase continuously (Fig. 5) from zero (isotropic rotational diffusion) to their values corresponding to the A equilibrium positions (without libration). We have represented in Fig. 6, in the $(1\bar{1}0)$ plane, the orientational probability of the molecular Δ axis, at 172 and 282 K. It can be seen that when the temperature decreases, the molecular Δ axis is more and more localized along the $\langle 111\rangle$ cubic-lattice axes. It is important to know if this molecular orientational probability is a good description of the reality. If we take into account the eight equilibrium positions (four of which are discernible) the isotropic librational mean-square amplitude deduced from this method is:

$$L_i = [16\pi C_\Delta(\langle 111\rangle)]^{-1}. \qquad (4)$$

The L_i values deduced from (4) are always higher than those obtained with the Frenkel model. This difference arises because the A^l_{m1} $(l>6)$ terms are not used in our refinements, as opposed to the Frenkel model which takes into account all the existing l orders. This hypothesis is verified by the fact that the difference between the two $\sqrt{L_i}$ determinations decreases from 4·2 to 2·6° when the temperature increases from 172 to 282 K.

If we suppose that order 10 is sufficient to describe the orientational probability, one can obtain an estimation of the A^8_{11} and A^{10}_{11} parameters. As we know the exact L_i value refined with the Frenkel model, we can deduce the correct value of C_Δ ($\langle 111\rangle$) with equation (4) and then the two previous terms can then be obtained [Amoureux *et al.*, 1981; equation (22)]. We have found that their relative evolution, with respect to their Frenkel values (without libration), is 0·9 at 172 K and 0·2 at 282 K. Therefore, we obtain $A^8_{11}\approx 0{\cdot}18$, $A^{10}_{11}\approx -0{\cdot}58$ at 172 K and $A^8_{11}\approx 0{\cdot}04$, $A^{10}_{11}\approx -0{\cdot}13$ at 282 K.

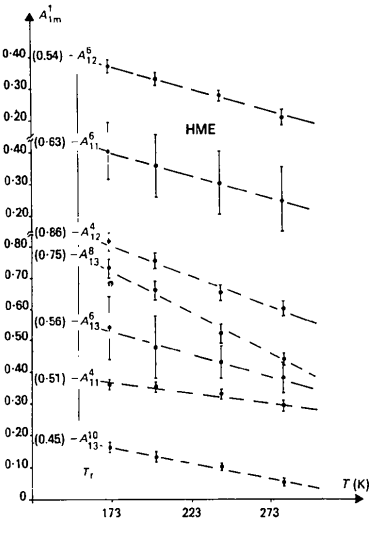

Fig. 5. $A^l_{1m'}$ values (with error bars) *versus* temperature for HME. We have also indicated in brackets the theoretical values corresponding to the 'equilibrium positions' deduced with the Frenkel model, without libration.

VI. Discussion

The structures of three similar compounds in their plastic phases (ethane, HME and HMDS) have been analysed by two different methods: a Frenkel model and a decomposition of the molecular orientational probability on symmetry-adapted functions. These two methods always lead to the same 'equilibrium positions' and to the same translational Debye–Waller factor. The molecules occupy four different equilibrium positions which correspond to an alignment of the molecular Δ and lattice $\langle 111\rangle$ threefold axes. Moreover, around these $\langle 111\rangle$ axes, they have only one equilibrium position: the six lateral C atoms (or H atoms for ethane) being in the $(1\bar{1}0)$ planes, close to the $\langle 001\rangle$ axes.

In the case of HME, the refinements have always been slightly better for the CALDER conformation than for the LEM one, particularly near the transition. We have tried to compare the advantages and disadvantages of the two different structural analyses.

The Frenkel model needs only a very small number of parameters with very simple significances. Its description of the reality is all the better as the molecular orientations are localized: the thermal motions are assumed to be harmonic.

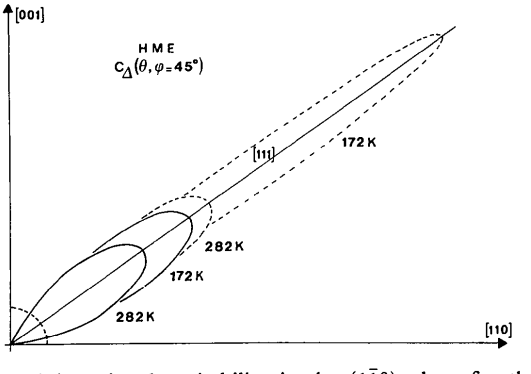

Fig. 6. Orientational probability in the $(1\bar{1}0)$ plane for the Δ molecular threefold axis of HME. The circle corresponds to the value $\frac{1}{4}\pi$ for a completely random distribution of orientations. Full curves correspond to the $A^l_{1m'}$ values of Table 3. Dashed curves are obtained by introducing in addition the calculated values: $A^8_{11}=-0{\cdot}18$, $A^{10}_{11}=-0{\cdot}58$ at 172 K and $A^8_{11}=0{\cdot}04$, $A^{10}_{11}=-0{\cdot}13$ at 282 K.

On the other hand, the method with symmetry-adapted functions always requires more parameters. Its use is mainly interesting when the molecular orientations are not really localized, because the librational anharmonicity is then taken into account. However, two problems may occur in this method which is available only for rigid molecules:

(i) When the translational amplitude is very important, as for HMDS, the Bragg reflections are only observable for small values, even if the molecular orientations are localized. It is then very difficult to deduce from the refinements the orientational molecular probability.

(ii) When the functions adapted to the molecular symmetry have negligible values for the atoms of the external shells of the molecule, the corresponding $A^l_{mm'}$ terms are only related to the internal shells and are not then easily refinable. In this case, occurring in HME, the molecular orientational probability deduced from the refinements is less localized than in reality, mainly at low temperature.

However, the comparative use of these two different methods gives a very accurate view of the long-range order in plastic crystals.

We would like to thank Professors Fouret and Lefebvre for their interest in this work and Drs Sauvajol, Gharby and Gors for interesting discussions.

References

ALBERT, S., GUTOWSKY, H. S. & RIPMEESTER, J. A. (1972). *J. Chem. Phys.* **56**, 1332-1336.
AMOUREUX, J. P., SAUVAJOL, J. L. & BEE, M. (1981). *Acta Cryst.* A**37**, 97-104.
BEE, M. (1985). Unpublished.
CHADWICK, A. V., CHEZEAU, J. M., FOLLAND, R., FORREST, J. W. & STRANGE, J. H. (1975). *J. Chem. Soc. Faraday Trans.* 1, pp. 1610-1622.
EGGERS, D. F. (1975). *J. Phys. Chem.* **79**, 2116-2118.
GHARBY, J., SAUVAJOL, J. L., FONTAINE, H. & MORE, M. (1985). *J. Raman Spectrosc.* **16**, 79-89.
MULLER, M. (1981). Thesis, CNAM, Lille.
PRANDL, W. (1981). *Acta Cryst.* A**37**, 811-818.
REYNOLDS, P. A. (1979). *Mol. Phys.* **37**, 1333-1348.
SCOTT, D. W., DOUSLIN, D. R., GROSS, M. E., OLIVER, G. D. & HUFFMAN, J. M. (1952). *J. Am. Chem. Soc.* **74**, 883-888.
SEYER, W. F., BENNET, R. B. & WILLIAMS, F. C. (1949). *J. Am. Chem. Soc.* **71**, 3447-3450.
SUGA, H. & SEKI, S. (1959). *Bull. Chem. Soc. Jpn*, **32**, 1088-1093.
VAN NES, G. J. H. & VOS, A. (1978). *Acta Cryst.* B**34**, 1947-1956.

Acta Cryst. (1986). B**42**, 84-90

Structural and Molecular-Orbital Study of the Furoxan Ring.* Structures of 3-Phenylfuroxan and 4-Phenylfuroxan and Comparison with Related Structures

BY M. CALLERI†

Dipartimento di Scienze della Terra, Università di Torino, Via San Massimo 22, 10123 *Torino, Italy*

G. RANGHINO

Istituto G. Donegani, Via Fauser 4, 28100 *Novara, Italy*

AND P. UGLIENGO AND D. VITERBO

Istituto di Chimica Fisica dell' Università, Corso M. D'Azeglio 48, 10125 *Torino, Italy*

(*Received* 4 *April* 1985; *accepted* 22 *July* 1985)

Abstract

Ab initio and CNDO/2 molecular-orbital calculations have been performed for the positional isomer pairs of phenylfuroxan, methylfuroxancarboxamide, isopropyl *N*-(methylfuroxanyl)carbamate, and chloro(phenyl)furoxan, for the molecules of dimethylfuroxan, diphenylfuroxan, and furazan and for an idealized unsubstituted furoxan molecule. The furoxan ring appears to be electron-overcrowded, in particular in furoxan itself, which has not been synthesized so far. This excess of charge is released toward the substituents in the derivatives. In all derivatives the furoxan group remains the most reactive part of the molecule. 3-Phenylfuroxan, (1*A*): $C_8H_6N_2O_2$, m.p. 380 K, $M_r = 162.1$, triclinic, $P\bar{1}$, $a =$ 6·438 (1), $b = 7{\cdot}017$ (2), $c = 9{\cdot}151$ (1) Å, $\alpha =$ 74·75 (1), $\beta = 72{\cdot}05$ (1), $\gamma = 82{\cdot}50$ (1)°, $U =$ 378·9 (1) Å^3, $Z = 2$, $D_x = 1{\cdot}42$ Mg m^{-3}, graphite-monochromatized Cu $K\alpha$ radiation, $\lambda = 1{\cdot}54178$ Å, $\mu = 0{\cdot}9$ mm^{-1}, $F(000) = 168$, room temperature, $R =$ 0·051 for 1254 independent diffractometer reflexions. 4-Phenylfuroxan, (1*B*): $C_8H_6N_2O_2$, m.p. 393 K, tri-

* Furoxan is furazan *N*-oxide.

† To whom correspondence should be addressed.

0108-7681/86/010084-07$01.50